

promoting access to White Rose research papers



Universities of Leeds, Sheffield and York
<http://eprints.whiterose.ac.uk/>

This is an author produced version of a paper published in **The International Journal of Advanced Manufacturing Technology**.

White Rose Research Online URL for this paper:
<http://eprints.whiterose.ac.uk/10433>

Published paper

Yusoff, A., Turner, M.S., Taylor, C.M., Sims, N.D. (2010) *The role of tool geometry in process damped milling*, The International Journal of Advanced Manufacturing Technology, Published Online 18th March 2010
<http://dx.doi.org/10.1007/s00170-010-2586-6>

The role of tool geometry in process damped milling

Ahmad R Yusoff · Sam Turner · Chris M Taylor · Neil D Sims

Submitted: 1 December 2009

Abstract The complex interaction between machining structural systems and the cutting process results in machining instability, so called chatter. In some milling scenarios, process damping is a useful phenomenon that can be exploited to mitigate chatter and hence improve productivity. In the present study, experiments are performed to evaluate the performance of process damped milling considering different tool geometries (edge radius, rake and relief angles and variable helix/pitch). The results clearly indicate that variable helix/pitch angles most significantly increase process damping performance. Additionally, increased cutting edge radius moderately improves process damping performance, while rake and relief angles have a smaller and closely coupled effect.

Keywords process damping · milling · chatter · tool geometry

Ahmad R Yusoff
Dept of Mechanical Engineering, University of Sheffield, Mappin Street, S1 3JD, UK

Sam Turner
Factory of the Future, Advanced Manufacturing Research Centre with Boeing, The University of Sheffield, Advanced Manufacturing Park, Wallis Way, Catcliffe, Rotherham S10 1GZ, UK

Chris M Taylor
Dept of Mechanical Engineering, University of Sheffield, Mappin Street, S1 3JD, UK

Neil D Sims
Dept of Mechanical Engineering, University of Sheffield, Mappin Street, S1 3JD, UK,
Tel.: +44 114 2227724
Fax.: +44 114 2227890
E-mail: n.sims@sheffield.ac.uk

1 Introduction

Regenerative chatter is the most common cause of instability in metal cutting, and this often limits the productivity of machining operations. Merritt [1] showed that regenerative chatter is caused by interaction between the structural dynamics of the machine tool and the dynamics of the cutting process. The requirement for high productivity leads to a desire to suppress chatter. Various methods have been proposed with this goal in mind. These include adding passive or active damping [2,3] spindle speed manipulation or variation [4,5] and alternative methods [6,7]. Besides the damping produced from the structure of machine tools, the machining process itself can add damping to the system through a phenomenon known as process damping.

The term process damping force or resistance force was introduced by Tobias and Fishwick [8]. They proposed that such forces occur when the tool flank or relief face rubs against the wavy workpiece surface at low spindle speeds. The stability diagram shown in Fig. 1 illustrates the relationship between spindle speeds, depth of cut and chatter stability. At high spindle speeds stability lobes can be observed, and this allows high productivity cutting to be performed on easy-to-machine materials such as aluminium alloys. Unfortunately the resulting high surface speeds are incompatible with more difficult-to-machine materials such as titanium and nickel based alloys. In this case, the practitioner is limited to low spindle speeds, where the chatter stability is strongly influenced by the process damping phenomenon. However, understanding of process damping remains an area for investigation in chatter research [9].

There have been many attempts to study process damping in turning operations using simulation or experimental methods (or both). Recent examples include [10] and [11]. However there have been fewer studies that have investigated milling processes. For example, Montgomery and

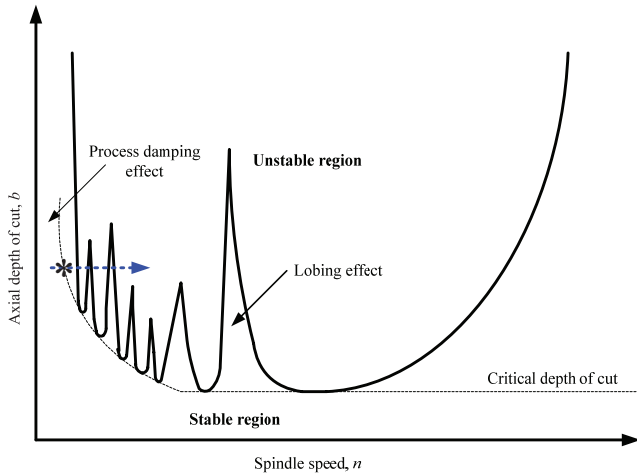


Fig. 1 Process damping stability lobe. The horizontal arrow represents a constant depth of cut with an increasing spindle speed, and the * marker shows the spindle speed at which process damping no longer prevents severe chatter.

Altintas [12] used a model-based approach to investigate ploughing forces. Delio *et al* [13] considered the wavelength of chatter vibration and the loss of process damping behaviour at higher spindle speeds. Elbestawi *et al* [14] modelled process damping effects when cutting aluminium and showed that the model could produce additional damping forces due to the tool flank / workpiece interference. Ranganath *et al* [15] also developed a time-domain model of process-damped milling and compared the results to experimental data from an aluminium alloy workpiece. Huang and Wang [16] proposed a model that considered the consequences of chatter vibration on the effective rake and relief angles. They included additional empirical parameters in their model so that the cutting stiffness became a function of these effective angles, and thereby produced a process damping effect.

Despite this previous work on process damping in milling, to the authors knowledge there has been limited experimental activity that has considered the effect of milling tool geometry when cutting difficult to machine materials such as titanium alloys. From a practical and industrial perspective, understanding the effect of these tool parameters on process damping is clearly of great importance, because it allows the practitioner to choose better tooling for specific machining problems. Consequently, the aim of the present study is to perform experimental milling trials so that different tool geometries (edge radius, rake and relief angles and variable helix/pitch angles) can be ranked in terms of their positive influence on process damping in milling.

The remainder of this manuscript is organised as follows. The process damping theory is first described, followed by the experimental procedure. Then, the results for the experiments are presented and parameters are ranked in

terms of their influence on process damping performance. Finally conclusions are drawn and recommendations for further work are made.

2 Theory of Process damping

Chatter is produced from self-excited vibration during cutting resulting in a high amplitude unstable motion. The amplitude of this motion is limited by nonlinearities such as tool loss of contact, nonlinear cutting force coefficients, and nonlinear stiffness of the machine tool structure. The chatter frequency is close to a natural frequency of the system. At low speeds the wavelength λ of these surface waves is much smaller, since the wavelength is proportional to surface velocity v and inversely proportional to regenerative vibration frequency f_c , as follows:

$$\lambda = \frac{v}{f_c} \quad (1)$$

As the spindle speed (and hence surface velocity) is reduced, the process damping phenomenon becomes sufficient for the regenerative chatter to be stabilised or suppressed. This situation is shown by the '*' marker (for a particular depth of cut) on Fig. 1. The corresponding surface vibration wavelength is given by Eq. (1), and is referred to as the process damping wavelength λ_c .

The commonly proposed mechanism of process damping is shown schematically in Fig. 2. As each tooth removes the chip from the wavy surface, process damping forces are generated that act on the structure. The damping force corresponds to inference between tool flank face and wavy surface, where more damping force occurs at point 'B'. A ploughing force can be produced from the workpiece being deformed by the tool, while the surface angle changes the effective shear angle of the tool. Interference is minimised when the tool travels upwards on the wave (position 'D' on Fig. 2) due to the positive slope of the machined surface.

According to this concept, low relief angles should produce high ploughing forces from the interference between tool and workpiece. Consequently, different rake and relief angles should be considered in the evaluation of process damping. Furthermore, Fig. 2 assumes a perfectly sharp tool, which is unrealistic in practice. Consequently the bluntness of the tool tip, which can be characterised as an edge radius, should also be considered.

In the stability of high speed milling, axial depth of cut b is the most influential factor, since the cutting forces are often considered to be given by the relationship

$$F = k_s b (Y_o - Y) \quad (2)$$

where F is the cutting force, b is the axial depth of cut, k_s the empirical cutting stiffness, and $(Y_o - Y)$ is the change in surface position between current and previous cuts. In theory,

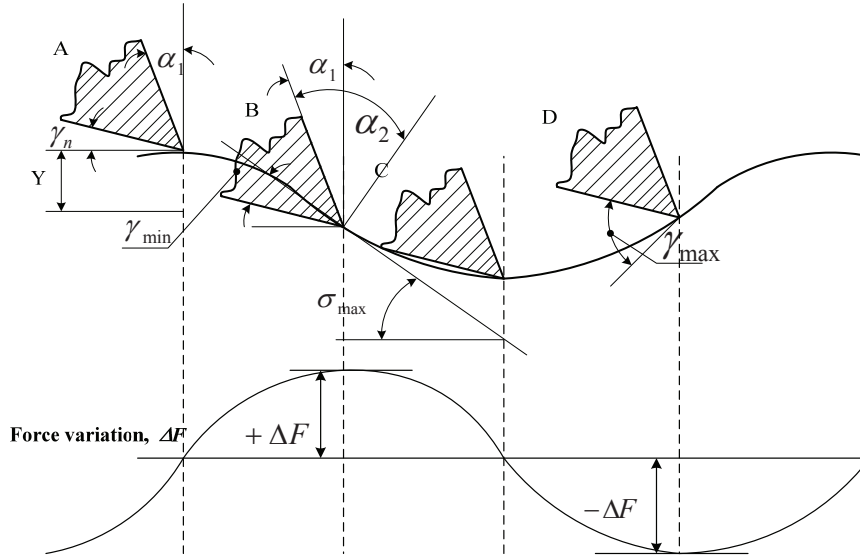


Fig. 2 Process damping mechanism. γ is the effective relief angle for a surface waveform of slope σ . The corresponding effective rake angle is α_2 , and the surface waveform amplitude is Y . The minimum effective relief angle occurs at location B, whilst the maximum value occurs at location D.

the stability boundary is then independent of the feed rate despite the influence of the feed rate on the mean chip thickness. In practice the empirical cutting stiffness k_s changes with the feed rate so that the feed rate does have some influence on the overall stability. However, under process-damped cutting conditions, the effect of feed rate has been observed to be more significant [17].

It is useful to express the feed rate in terms of the maximum chip thickness h_{max} [18]:

$$h_{max} = fpt \sqrt{\frac{4r}{D} - \left(\frac{2r}{D}\right)^2} \quad (3)$$

Here, r is the radial immersion of the tool, and D is the tool diameter. The feed per tooth fpt is related to the machining feed rate f , number of teeth m and spindle speed n by:

$$f = m \times fpt \times n \quad (4)$$

Using a high depth of cut at low cutting speed results in the chatter stability being dominated by process damping effects, as shown at the left side of the stability diagram in Fig. 1. Meanwhile, using a low radial immersion helps to reduce the total machining forces and improve tool life. This approach will be employed in the present study in order to determine the process damping wavelength λ_c under different tool geometry and feed rate conditions.

3 Experimental Setup

Two experimental configurations were used in this study, and these will now be introduced. It should be pointed out

that the majority of experiments were performed on difficult-to-machine titanium alloy, where process damping is frequently encountered. These tests involved a 4 flute tool that was considered to be the flexible component in the machine-tool system. However, this configuration does not allow quantitative acceleration data to be collected, because the flexible component is the rotating cutting tool. Consequently one set of data, using three flute regular helix and variable helix tools, was collected using a workpiece mounted on a flexure. This also ensured that the tool helix angle did not influence the relevant modal parameters of the system. However, the extreme flexibility of the flexure configuration meant that an easier-to-machine workpiece material (aluminium alloy) was needed for this set of tests.

3.1 Flexible tool condition

For the flexible tool setup, 16 mm 4 flute solid carbide tools were used to cut titanium $Ti_6 Al_4 V$ to evaluate the influence of feed rate, tool edge radius, rake angle, and relief angle on process damping. Before the machining test, each tool was measured to determine the average edge radius using a Mahr Perthometer with a stylus tip. One edge from four was selected to measure the cutting edge radius. With reference to Fig. 3, the cutting edge radius was measured at 3 mm from the bottom and the middle of the depth of cut (b). The measurement was repeated 3 times and then repeated at the same location for the second, third and fourth flutes (Fig. 3b) counted clockwise from the bottom.

The experiment was started by determining the frequency response function (FRF) of the tool to identify the expected dominant chatter frequency for initial selection of the spin-

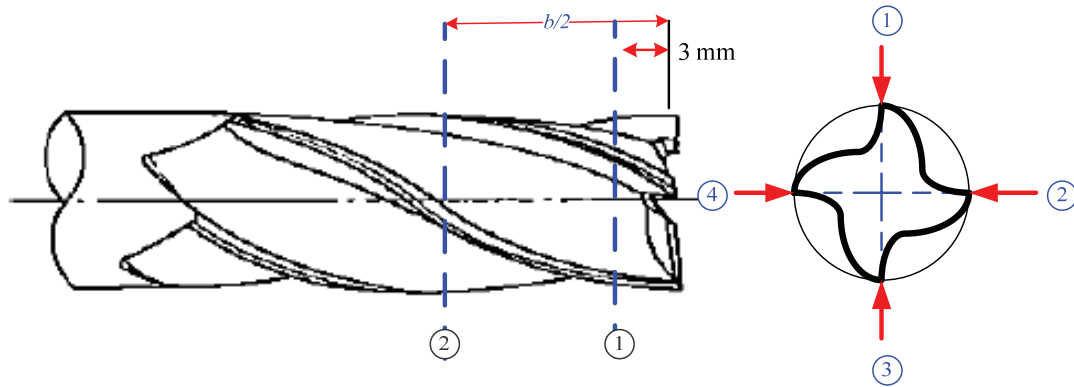


Fig. 3 Milling tool measurement location, for tests described in Section 3.1.

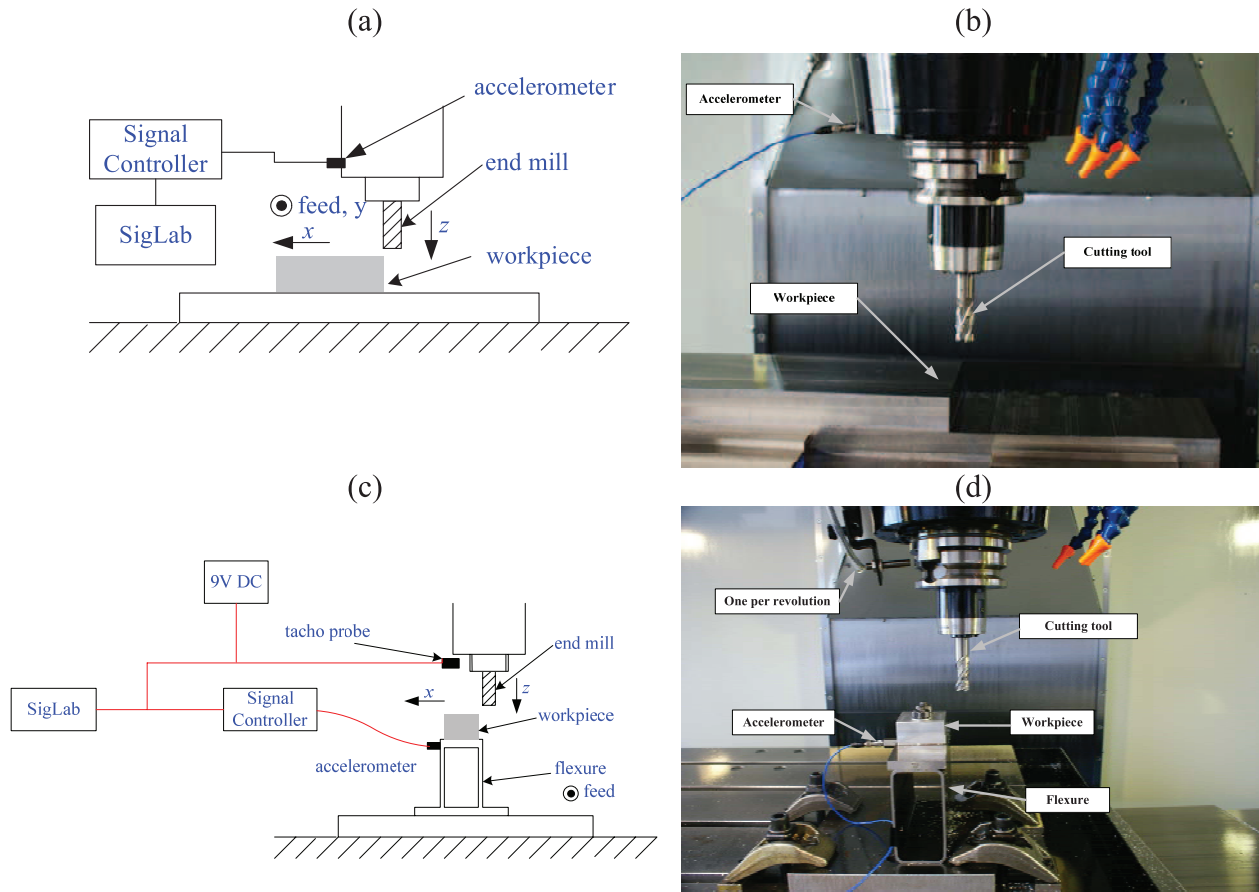


Fig. 4 Experimental process damping arrangement. (a) Schematic diagram of flexible tool (b) Sensor location of flexible tool (c) Schematic diagram of flexible workpiece (d) Sensor location of flexible workpiece

dle speed and feed rate. A normal force was applied at the tool tip using a PCB 086C01 modal hammer with steel tip. The acceleration response was taken by a PCB Piezotronics 352C68 accelerometer opposite to the hammer impact point. A Siglab 20-22A two-channel data acquisition system was connected to the hammer and accelerometer to determine the frequency response function (FRF).

From the FRF, the resonant frequency was used to choose a starting value for spindle speed so that the expected wavelength of vibrations was $\lambda = 0.1$ mm. This was achieved using Eq. (1) and the relationship between tool diameter, spindle speed, and surface speed. Based upon previous experience [19] this initial wavelength was expected to be below the process damping wavelength λ_c . For the desired maxi-

mum chip thickness, the feed per tooth and hence the initial feed rate were then determined using Eq. (3) and Eq. (4). A low radial width of cut ($r = 1$ mm) and large axial depth of cut ($b = 30$ mm) were used to minimise forced vibration, reduce tool wear, and prevent damage to the tool if severe chatter occurred.

Machining was performed on a Haas VF6 vertical milling machine, as shown in Fig. 4a. During cutting, the vibration signal was recorded using an accelerometer. The spindle speed n and feed rate f were incremented simultaneously to maintain constant f_{pt} and h_{max} , until chatter was detected. Process damping performance was then evaluated in terms of λ_c from Eq. (1). Here, the chatter frequency was obtained from Fourier analysis of the vibration signal, and the surface speed v was determined based upon the spindle speed at which chatter occurred.

The procedure was repeated for four h_{max} values between 0.03mm and 0.1mm, and for each tool.

3.2 Flexible workpiece condition

A separate sequence of experiments was performed to evaluate the influence of variable pitch and helix angles on process damping performance. Here, a block of aluminium (7075-T6) was mounted on a flexible structure as used by Huyanan and Sims [20, 21] (Fig. 4c and d). Two 16 mm three flute cutters were used: one with a regular pitch and uniform helix ($30^\circ, 30^\circ, 30^\circ$), and one with a variable pitch ($84^\circ, 221^\circ, 55^\circ$) and variable helix ($43^\circ, 44^\circ, 48^\circ$). These cutters are shown in Fig. 5.

A similar procedure was followed to determine the initial spindle speed and feed rate based upon the FRF of the flexure. Again, the spindle speed was gradually increased whilst maintaining the feed per tooth until chatter was detected. The process damping wavelength λ_c was then evaluated as before. Both regular and variable helix/pitch milling tools were used for down-milling at 1 mm radial and 2 mm axial depth of cut. The low stiffness of the flexure ensured process damped cutting conditions despite the low axial depth of cut. Due to the aluminium being easier to machine than the titanium workpiece, four values of maximum chip thickness h_{max} from 0.04 mm to 0.12 mm were used. Flexure acceleration was detected using an accelerometer as shown in Fig. 4c. In addition, a hall-effect probe triggered by two equally spaced slots on the tool holder was used (Fig. 4c,d) to measure the spindle rotation. This allowed once per revolution samples (1/rev) and two-dimensional Poincaré maps to be constructed [22] so as to illustrate the nonlinear response. Stable behaviour was detected from 1/rev accelerometer samples approaching a fixed point with a variance less than 10^{-3} . The procedure was repeated for each of the h_{max} values for regular and variable helix/pitch tools.

4 Results

The results of both experimental configurations will now be presented to investigate the influence of tool geometry on process damping performance. First, edge radius measurements, and FRFs of the tool and workpiece are presented. Repeatability tests are then shown in order to include a basic error analysis in the main experimental results.

4.1 Preliminary tests

The measurements of the cutting edge radius of the tools are first presented in Table 1. The relatively high standard deviations indicate that the edge radius varied somewhat between the measurements on individual tools. Nevertheless, there is a significant variation in edge radius between one tool and the next. This allows the process damping performance to be characterised in terms of the tool's average edge radius.

Table 1 Milling tool geometry

Tool	Rake angle α (deg)	Relief angle γ (deg)	Average cutting edge radius, (μm) (and standard deviation)		
			Tool 1	Tool 2	Tool 3
PD5	0	6	16.9(7.8)	9.9(2.6)	8.3(3.1)
PD6	0	12	11.4(5.4)	12.8(3.7)	13.5(3.3)
PD8	6	6	9.7(4.6)	12.8(3.6)	12.4(5.2)
PD9	6	12	9.3(2.5)	7.1(1.9)	8.2(2.0)
PD11	12	6	8.0(1.5)	11.4(3.4)	17.0(8.3)
PD12	12	12	10.8(2.4)	7.1(3.0)	10.8(3.0)

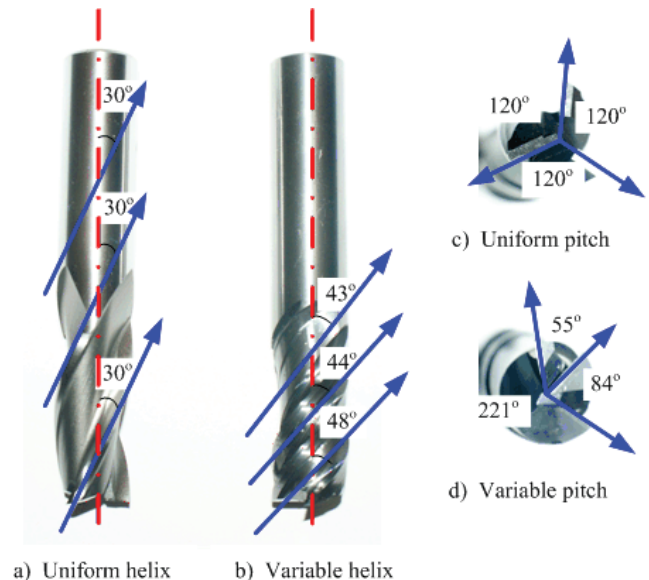


Fig. 5 Tool geometry for the flexible workpiece experiments (Section 3.2).

As previously mentioned, the FRF of the tools was used to select initial values for the spindle speed and hence feed rate. The FRF measurement is shown in Fig. 6a, where 2358 Hz is the major resonant frequency of the tool. The FRF was found to be very similar for all the tools used in the flexible tool experiments, and so only one set of data is included here. Using the procedure previously described, the required initial feed rate and spindle speed was determined. This led to an initial spindle speed of $n = 281$ rpm, and at $h_{max} = 0.03$ mm and initial feed rate $f = 70$ mm. A similar procedure was repeated for other h_{max} and tools.

Fig. 6b shows the frequency response function for the flexible aluminium workpiece used in the second experimental configuration. Here, a single resonant frequency is observed at 200 Hz. For these tests, the use of a flexible workpiece has avoided the issue of the tool helix angle influencing the dominant modal parameters of the system.

In the machining experiments, the spindle speed was increased smoothly and continuously under constant feed per tooth, until chatter was found. A typical result to demonstrate this method is shown in Fig. 7. Here, the accelerometer signal is plotted for multiple regions over the duration of the cut. Near the beginning of the cut (Fig. 7a), the vibration level is very low. As the spindle speed is increased (Fig. 7b and c) the vibration magnitude starts to grow, and a Fourier analysis indicates that the peak frequency is close to the natural frequency of the tool. Eventually the vibration magnitude at the chatter frequency is deemed unacceptable (Fig. 7d). Based upon this result, the corresponding process damping wavelength can then be determined. A corresponding image of the workpiece surface is shown in Fig. 7e. This procedure was repeated for each cutter, for four different values of maximum chip thickness.

Clearly the procedure outlined above is somewhat subjective because it involves an arbitrary threshold for determining the onset of chatter vibrations of an unacceptable amplitude. Furthermore, small variations in the setup from one experiment to the next could have an influence on the observed behaviour. Consequently, at the end of the experiments, a selection of tests were repeated to assess the influence of process variability, and also to confirm that the threshold-based analysis approach gave consistent results. Performing the repeated tests after the other experiments also meant that there would be a slight amount of tool wear, so the influence of this wear could be compared to the influence of the other process parameters. Some repeatability tests are presented in Fig. 8. It can be seen that all tools indicate a repeatability error of less than ± 5 percent between the original test/analysis and the repeated test/analysis. It is clear that even considering this repeatability error, the maximum chip thickness (and consequently the feed per tooth) has a very significant effect on the process damping wavelength.

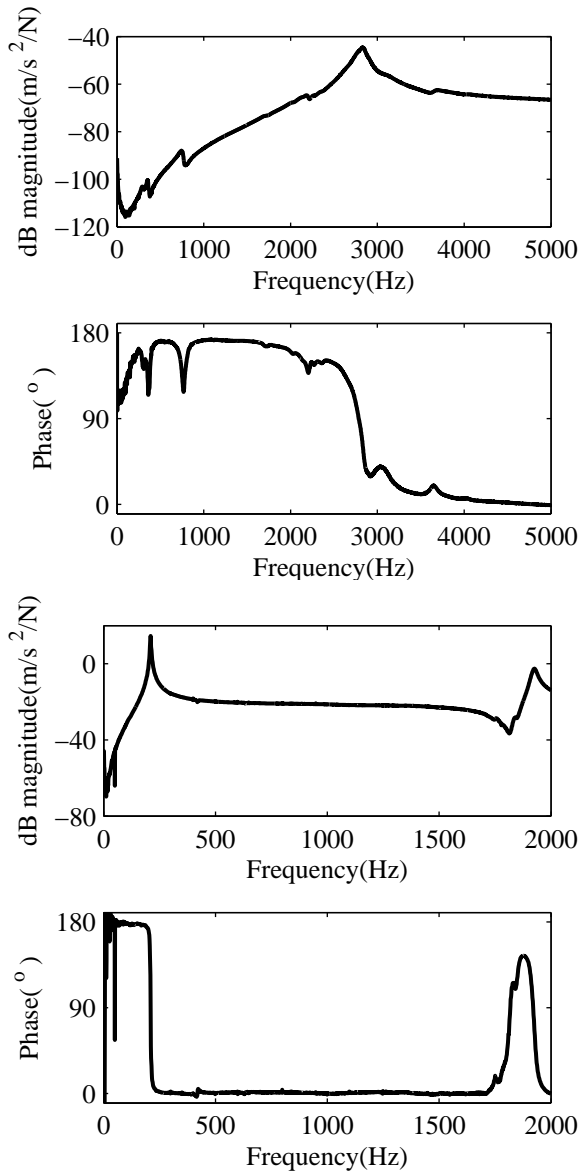


Fig. 6 Typical frequency response function. a) PD5 tool 1 in x-direction. b) Flexure in x-direction.

A further check on the accuracy of the data involved a comparison with previous tests [17] that were performed using the same tool and workpiece specifications. In these earlier experiments, tool edge measurement facilities were not available, and the process damping wavelength was determined only for $h_{max} = 0.03$ mm. Nevertheless there was reasonable agreement between the two sets of data.

Consequently, in the following sections the role of tool geometry will be considered, using error margins of $\pm 5\%$ on the experimental data.

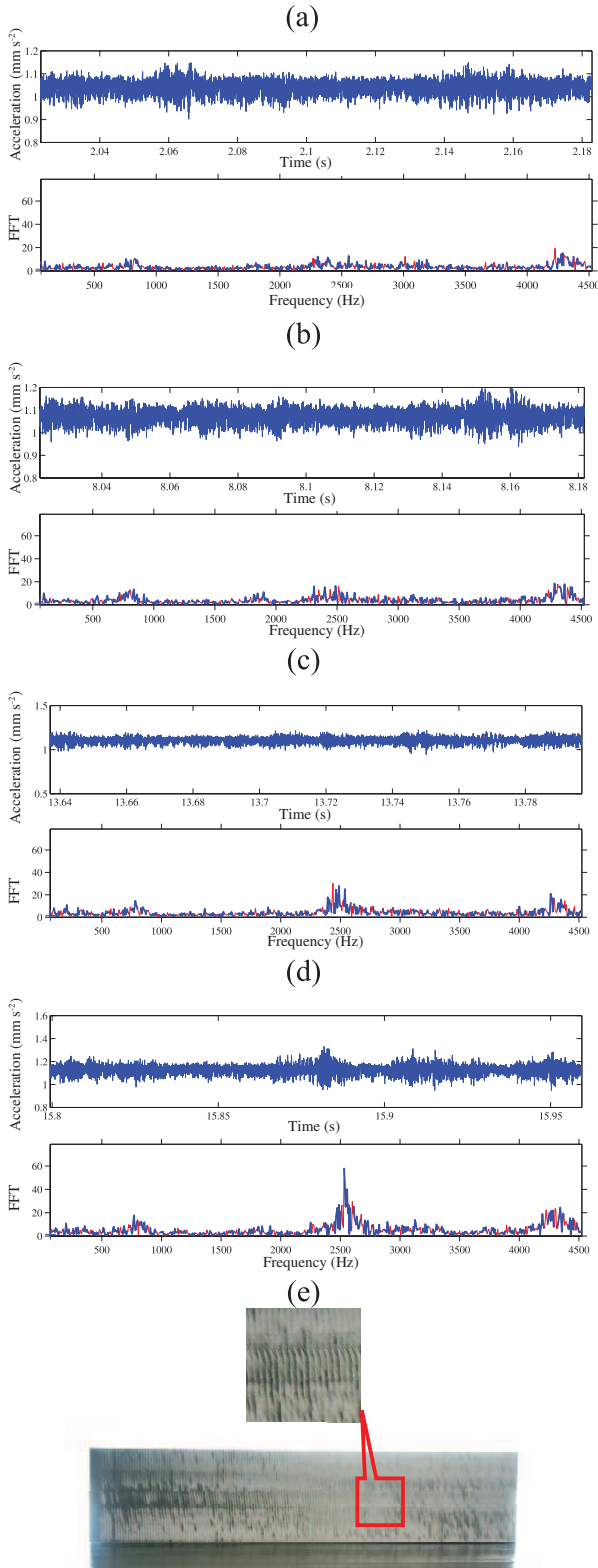


Fig. 7 FFT level and workpiece surface for PD11 tool 3 at $h_{max}=0.075\text{mm}$. (a) Stable condition with $n = 281$ rpm and $f = 174$ mm/min. (b) Stable condition with $n = 309$ rpm and $f = 262$ mm/min. (c) Stable condition with $n = 340$ rpm and $f = 289$ mm/min. (d) Chatter detection with $n = 374$ rpm and $f = 317$ mm/min (e) Workpiece surface at condition (c).

Table 2 Classification of tool edge radius

Classification Range (μm)	Low 6-10	Medium 11-15	High 16-20
PD5	Tool 2,3		Tool 1
PD6		Tool 1,2,3	
PD8	Tool 1	Tool 2,3	
PD9	Tool 1,2,3		
PD11	Tool 1	Tool 2	Tool 3
PD12	Tool 2	Tool 1,3	

4.2 Cutting edge radius

Fig. 9 shows the process damping performance results for all tools. It can be seen that tools with identical rake and relief geometries have different process damping performance due to the edge radius of the tool. In all cases, the process damping performance improves when the cutting edge radius is increased. In some cases this variation was as significant as that obtained due to change in the maximum chip thickness. However, for some tools, particularly PD8, the change in edge radius has a marginal effect compared to the magnitude of the experimental error. Closer inspection reveals that tool PD8 had similar edge radii for all three tools, and the standard deviation for individual tools was also high. Consequently the fact that all three PD8 tools had similar performance is less surprising.

4.3 Rake and relief angles

In comparison to Section 4.2, the task of assessing the influence of tool rake and relief angle is more complex. In order to isolate the effect of tool rake and relief angle from the tool edge radius, the tools were first re-classified in terms of their edge radius. Three groups were formed based upon a low ($5\text{-}10\ \mu\text{m}$), medium ($11\text{-}15\ \mu\text{m}$) and high ($16\text{-}20\ \mu\text{m}$) edge radius. These groupings are shown in Table 2. It can be seen that only two tools, PD5(2) and PD11(4), were classified as having a high edge radius. Nevertheless, based on this classification, it is possible to compare tools that have a similar edge radius but different rake and relief angles.

In Fig. 10, a comparison of λ_c is made according to the average cutting edge radius classification, and a clear pattern can be seen. Fig. 10 shows that process damping performance decreased when the rake angle was increased for a relief angle of 6 degrees. In contrast, process damping performance increased when the rake angle was increased for a relief angle of 12 degrees (Fig. 10b,d). Again, this variation was more significant than the 5 percent repeatability error of the experiment. To summarise, a low relief angle gave better process damping performance with smaller rake angles, while at high relief angles, better performance is obtained

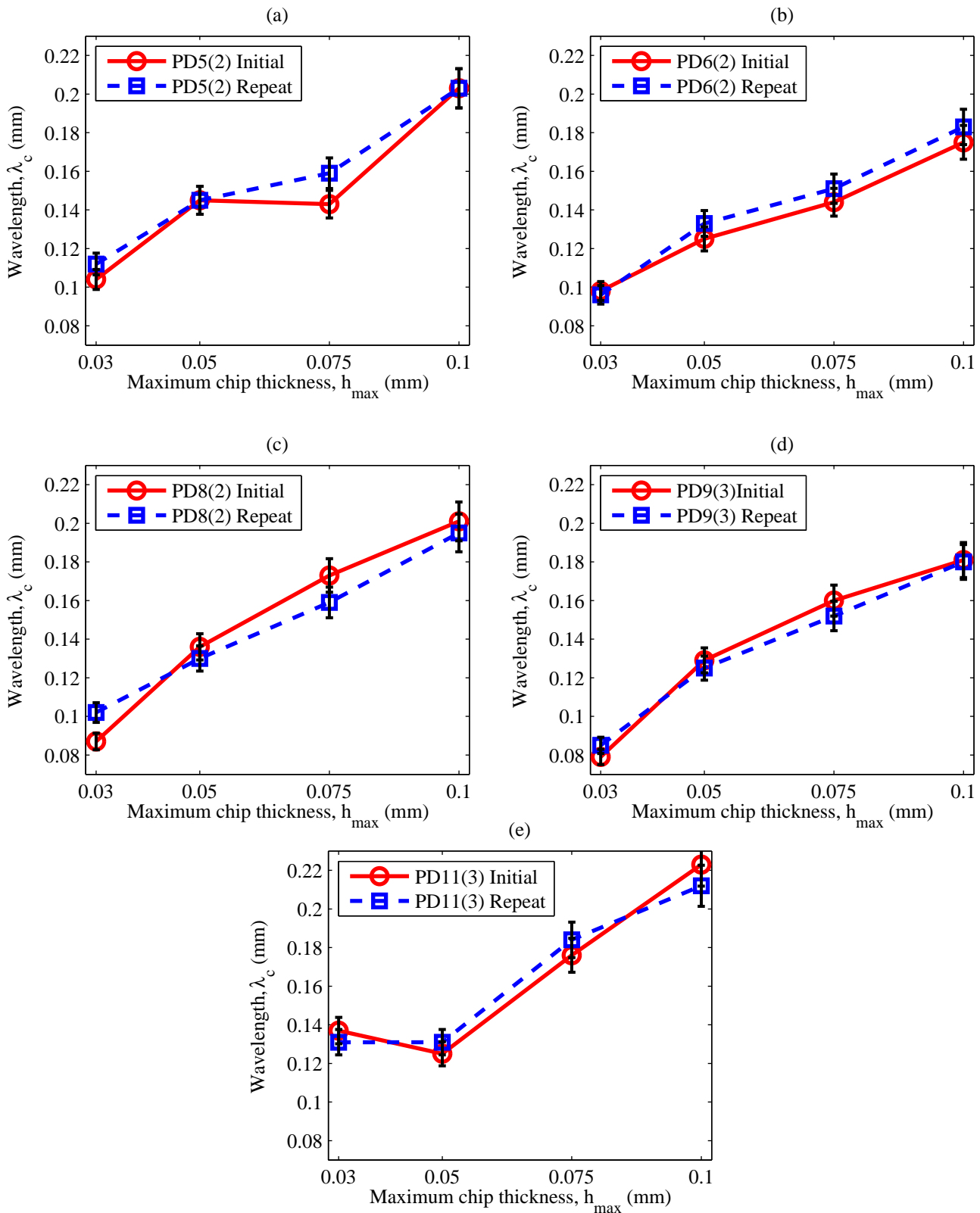


Fig. 8 Repeatability of selected tools. (a) PD5, tool 2; (b) PD6, tool 2; (c) PD8, tool 2; (d) PD9, tool 3, (e) PD11, tool 3

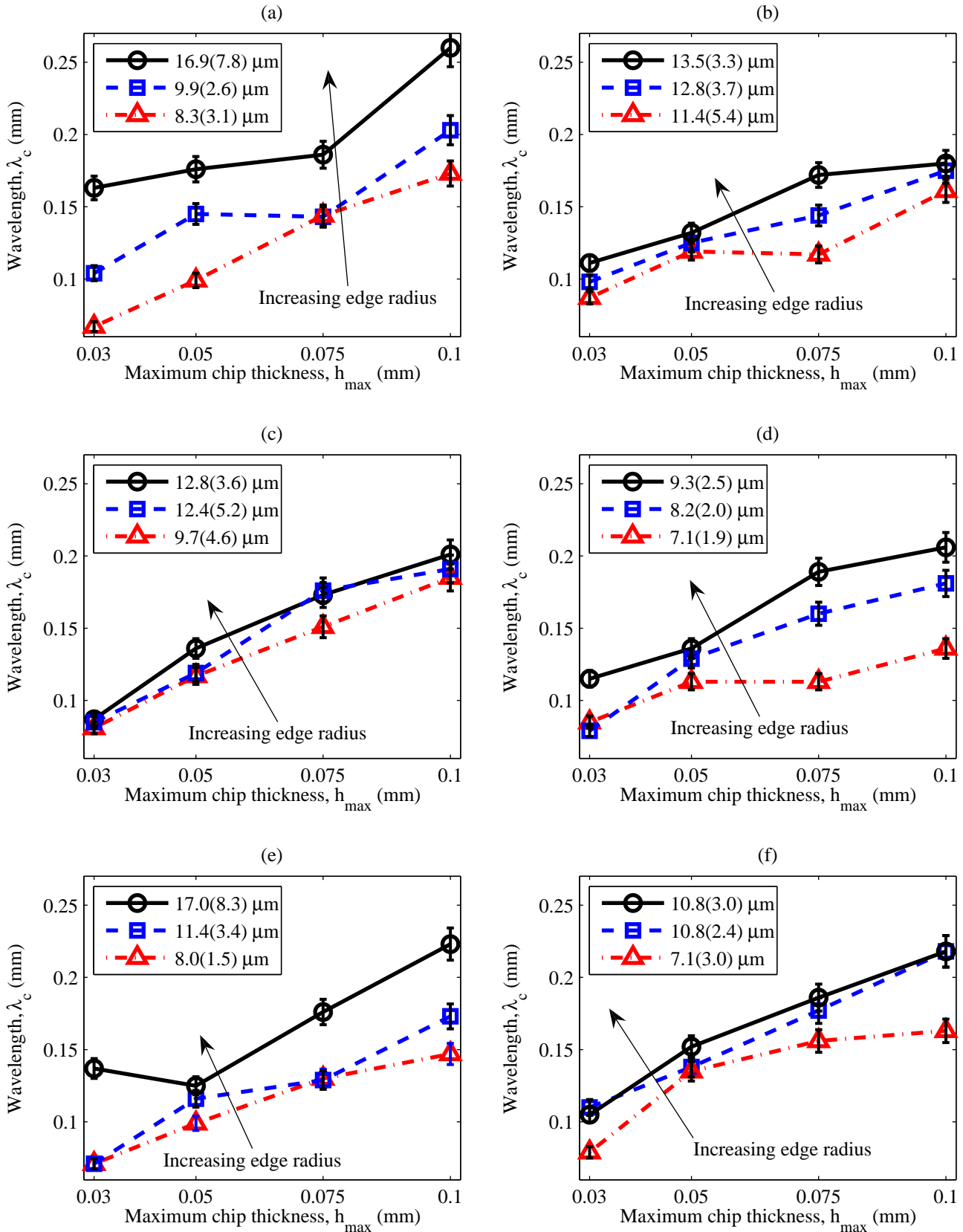


Fig. 9 Effect of tool edge radius on process damping wavelength. (a) PD5; (b) PD6; (c) PD8; (d) PD9; (e) PD11; (f) PD12

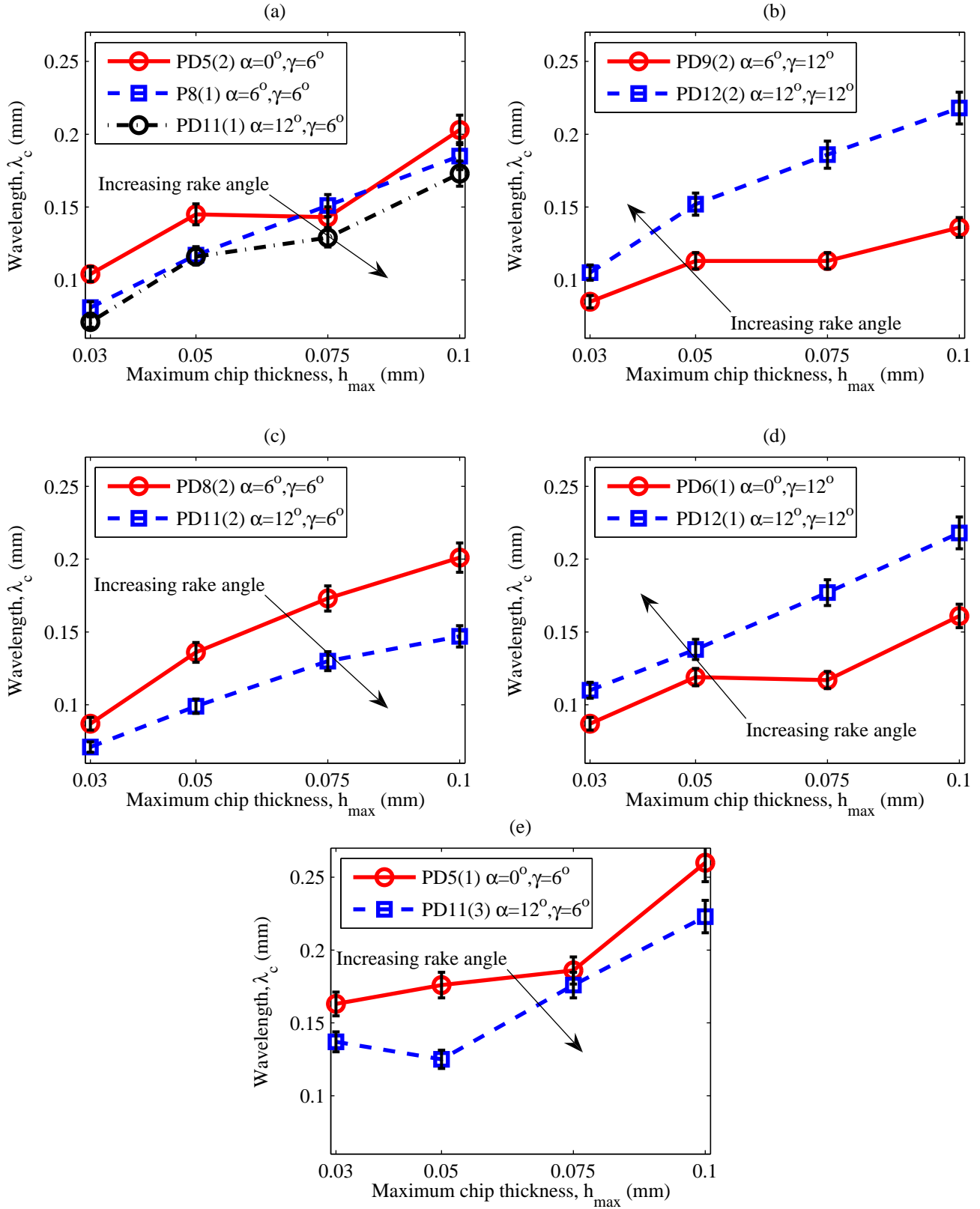


Fig. 10 Effect of rake and relief angles on process damping wavelength.
(a) Low edge radius at $\gamma = 6^\circ$; (b) Low edge radius at $\gamma = 12^\circ$
(c) Medium edge radius at $\gamma = 6^\circ$; (d) Medium edge radius at $\gamma = 12^\circ$
(e) High edge radius at $\gamma = 6^\circ$.

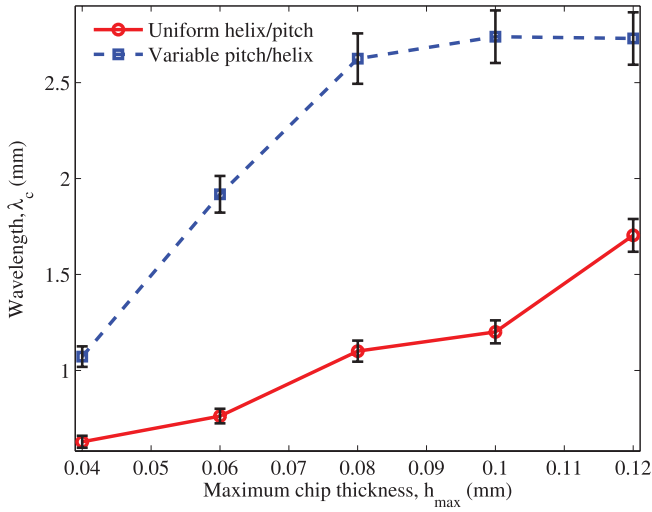


Fig. 11 Effect of variable helix and pitch angles on process damping wavelength

with higher rake angles. This was true for all the available edge radius classifications.

4.4 Variable helix/pitch angles

Regular and variable helix/pitch cutters were evaluated and their process damping performance compared as shown in Fig. 11. It should be re-iterated that this experiment concerned the machining of an aluminium alloy block on a very flexible workpiece. Consequently the measured process damping wavelengths were markedly different to the previous experiment (involving a titanium workpiece). In fact the process damping wavelength for this study was an order of magnitude greater. This could be attributed to the different workpiece material or the considerably lower axial depth of cut used in these experiments. Despite this, Fig. 11 shows the variable helix/pitch tool has a very high process damping wavelength compared to the standard tool. In fact, the process damping wavelength is almost doubled, which is a far more significant effect than that of the tool geometries considered in the previous experiment.

It is worth pointing out that the measurements obtained in the flexible workpiece experiments allow a more detailed and less subjective analysis of the vibrations, based upon once-per-revolution samples of the accelerometer signal. However, this advantage is at the expense of requiring easy-to-machine workpiece material (aluminium rather than titanium alloy), and a very low depth of cut.

5 Discussion

The results have demonstrated some interesting and useful relationships between tool geometry and processing damp-

ing performance. A number of issues are worthy of further discussion.

The experimental data shown in Fig. 7 indicate that the vibration during machining has grown quite steadily as the spindle speed was increased. This makes it difficult to identify a discrete transition from stable cutting to unstable cutting (i.e. chatter). Conversely at high spindle speeds previous experiments [13] and models [23] usually suggest a swift transition from stable to unstable cutting. The gradual increase in vibration amplitude observed in the present experiments has two implications. First, this indicates that the process damping phenomenon has a complex influence on the chatter stability boundary, since there is no clearly definable transition from stable machining (with low vibration amplitude) to unstable machining (with excessively high vibration amplitude). This is in contrast to the early work on ‘dynamic cutting force coefficients’ [8] which implies that there is a clearly defined stability boundary even under process damped cutting conditions. Second, the gradual growth in vibrations makes it more difficult to determine reliably the boundary between acceptable and unacceptable cutting that is indicated by the process damping wavelength. In the first set of experiments this issue was addressed by performing repeatability tests. In the second set of experiments the use of a flexible workpiece enabled a more quantitative analysis of the machining vibrations based upon the variance of the once-per-revolution acceleration samples. Clearly, the quantification and classification of processed damped milling performance remains an issue for further research.

Another issue for discussion is the possible mechanisms that have given rise to the behaviour observed in these experiments. Considering the influence of feed rate, it is clear that increasing the maximum chip thickness has increased the tool’s penetration into the workpiece. It could be argued that such changes in chip thickness could exacerbate any nonlinearity in the cutting force coefficients. However, a related set of experiments [17] suggests that this was not the case here. Consequently, alternative explanations are needed to explain the significant increase in process damping performance that is obtained by increasing the feed rate.

Meanwhile, the influence of tool edge radius is more readily explained by returning to the conceptual explanation illustrated in Fig. 2: if this figure were redrawn to include a tool radius, then flank/workpiece interference and tool/workpiece ploughing would clearly be increased. However, the complex interaction between rake and relief angle, along with their smaller influence on process damping performance cannot be explained by Fig. 2. Likewise, the dramatic influence of variable pitch/helix angles cannot be easily explained. To summarise, the focus of this study has been to illustrate experimental observations of process damped milling. Further work is needed to explain some of these

findings using realistic models of milling dynamics and chip mechanics.

The present study has focussed on the role of the tool's angular geometry in process damping, but the maximum chip thickness has also been considered, and this was varied by increasing the machining feedrate. In practice, the chip thickness is also a function of tool diameter and machining radial immersion, as shown in Eq. (3). Further work could investigate whether varying the tool radial immersion:diameter ratio has an equivalent effect to varying the machining feedrate. However, in practice other factors may influence the chosen radial immersion. For example, tool life is a critical factor under process damped conditions, and for a given material removal rate tool wear can be spread across more of the tool's length by using a large axial and low radial immersion.

It is useful to briefly compare the findings of this study with some of the previous literature on process damped turning and milling that has considered tool geometry. Much of the earlier research has considered easy-to-cut-materials (steel and aluminium), whereas the present study used titanium alloy when considering the tool rake, relief, and edge radius. Additionally, previous studies concerning increased edge radius have often focussed on turning operations. In turning experiments, Budak and Tunc [11] identified similar results concerning the edge radius, along with increased performance from a low relief angle and smaller rake angles. However, the present study has also indicated that high relief angles coupled with higher rake angles can contribute to better performance. Furthermore, to the authors' knowledge previous studies have not considered the role of variable helix/pitch angles on process damping behaviour.

Finally, as with any experimental investigation of machining chatter and process damping, the issue of experimental accuracy and repeatability needs to be properly considered before drawing conclusions from the collected data. In the present study, these experimental errors were addressed as follows. First, measurement and classification of tool edge radius involved an average of 12 measurements for each tool. Second, of the 18 tools that were tested, 5 were subjected to a repeat test as described in Section 4.1. The repeatability tests showed variations of less than 5 percent, and so appropriate error bars were included in the subsequent analysis. Third, a subset of experiments involved a repetition of previous tests that were reported in [17]. There was close agreement between the data sets, despite the use of different experimental equipment and different operating personnel. Consequently, the authors have sufficient confidence in the present results to draw general and industrially relevant conclusions from the data. Nevertheless, future efforts to provide a more statistically detailed analysis would be of value, particularly from a modelling and model calibration perspective.

6 Conclusion

This contribution has presented experimental results demonstrating the influence of edge geometry, rake and relief angles and variable helix/pitch angles on process damping performance in low speed milling. It has been revealed that under the selected conditions variable helix/pitch angles played a more significant role in increasing performance, compared to cutting edge, rake and relief angles, and feed rate. Increasing the edge radius also tended to increase the process damping performance to a significant extent. This has important implications because of the difficulties in controlling edge radius during tool manufacture, and the inevitable influence of tool wear on the tool edge geometry.

The effect of rake and relief angles was less significant and more complex. A low relief angle tool increased process damping performance when the rake angle was also low. However, for high relief angles, better performance was achieved with high rake angles. Both of these parameters were less significant than the variations in maximum chip thickness that were used in the present study.

From a practitioner's standpoint, these conclusions can be used to make informed decisions regarding tool choices, when other constraints require low-speed milling to be employed. In particular, variable helix/pitch tooling should be considered, as well as using a high feed rate. Inconsistent behaviour between nominally identical tools could be attributed to poor control of the tool's edge geometry, due to either manufacturing variability or tool wear.

Further work is needed to explain these trends with physically realistic models of process damped milling. Finally, it should be re-iterated that the present study benchmarked variable helix/pitch tools using a flexible aluminium workpiece rather than a rigid titanium workpiece. Further experiments are needed to investigate the performance of these tools when cutting titanium and other difficult-to-cut materials.

Acknowledgements Authors extend their sincere thanks to the support of the EPSRC (EP/D052696/1), Advanced Manufacturing Research Centre with Boeing at the University of Sheffield, and Technicut Limited. ARY is grateful for PhD studentship sponsored by Ministry of Higher Education of Malaysia and Universiti Malaysia Pahang.

References

1. H. E. Merritt. Theory of self-excited machine tool chatter, contribution to machine-tool chatter research-i. *Transaction ASME Journal of Engineering Industry*, 87(4):447–454, 1965.
2. Y. Zhang and N. D. Sims. Milling workpiece chatter avoidance using piezoelectric active damping: a feasibility study. *Smart materials and structures*, 14:65–70, 2005.
3. A. Ganguli, A. Deraemaeker, and A. Preumont. Regenerative chatter reduction by active damping control. *Journal of Sound and Vibration*, 300(3-5):847, 2007.

4. E. Soliman and F. Ismail. Chatter suppression by adaptive speed modulation. *International Journal of Machine Tools and Manufacture*, 37(3):355, 1997.
5. Y. S. Liao and Y. C. Young. A new on-line spindle speed regulation strategy for chatter control. *International Journal of Machine Tools and Manufacture*, 36(5):651, 1996.
6. Nejat Olgac and R. Sipahi. Dynamic and stability of variable pitch milling. *Journal of Vibration and Control*, 13(7):1031–1043, 2007.
7. N. D. Sims, B. Mann, and S. Huyanan. Analytical prediction of chatter stability for variable pitch and variable helix milling tools. *Journal of Sound and Vibration*, 317(3-5):664–686, 2008.
8. S. A. Tobias and W. Fishwick. Theory of regenerative machine tool chatter. *The Engineer*, 205:199–203, 1958.
9. Y. Altintas and M. Weck. Chatter stability of metal cutting and grinding. *CIRP Annals - Manufacturing Technology*, 53(2):619–642, 2004.
10. Y. Altintas, M. Eynian, and H. Onozuka. Identification of dynamic cutting force coefficients and chatter stability with process damping. *CIRP Annals - Manufacturing Technology*, 57(1):371–374, 2008.
11. E. Budak and L. T. Tunc. A new method for identification and modeling of process damping in machining. *Journal of Manufacturing Science and Engineering*, 131(5):051019, 2009.
12. D. Montgomery and Y. Altintas. Mechanism of cutting force and surface generation in dynamic milling. *Transaction ASME Journal of Engineering Industry*, 113:160–168, 1991.
13. T. Delio, S. Smith, J. Tlusty, and C. Zamudio. Stiffness, stability, and loss of process damping in high speed machining : , fundamental issues in machining, vol ped 43, dallas, tx, 1990. pp. 171–191. asme, new york, ny. *Precision Engineering*, 13(3):236, 1991.
14. M. A. Elbestawi, F. Ismail, R. Du, and B. C. Ullagaddi. Modelling machining dynamics including damping in the tool-workpiece interface. *Transaction ASME Journal of Engineering Industry*, 116(4):435–439, 1994.
15. S. Ranganath, K. Narayanan, and J. W. Sutherland. The role of flank face interference in improving the accuracy of dynamic force predictions in peripheral milling. *Journal of Manufacturing Science and Engineering*, 121:593–599, 1999.
16. C. Y. Huang and J. J. Junz Wang. Mechanistic modeling of process damping in peripheral milling. *Journal of Manufacturing Science and Engineering*, 129(1):12–20, 2007.
17. S. Turner. Process damping parameters. In *Trends in Aerospace Manufacturing 2009 International Conference (TRAM '09)*. Sheffield, 2009.
18. J. Tlusty. *Manufacturing Process and Equipment*. Prentice Hall, New Jersey, 2000.
19. T. R. Sisson and R. L. Kegg. An explanation of low speed chatter effects. *Transaction ASME Journal of Engineering Industry*, 91(4):951–956, 1969.
20. S. Huyanan and N. D. Sims. Active vibration absorbers for chatter mitigation during milling. In *Proc Ninth International Conference on Vibrations in Rotating Machinery 2008*, pages 125–140. University of Exeter, 2008.
21. Satiengpong Huyanan and Neil D. Sims. Vibration control strategies for proof-mass actuators. *Journal of Vibration and Control*, 13(12):1785–1806, 2007.
22. L. N. Virgin. *Introduction to experimental nonlinear dynamics: A case study in mechanical vibration*. Cambridge University Press, New York, 2000.
23. N. D. Sims. The self-excitation damping ratio: A chatter criterion for time-domain milling simulations. *Journal of Manufacturing Science and Engineering, Transactions of the ASME*, 127(3):433–445, 2005.